Hesperidin Attenuates Ultraviolet B-Induced Apoptosis by Mitigating Oxidative Stress in Human Keratinocytes

Susara Ruwan Kumara Madduma Hewage[1], Mei Jing Piao[1], Kyoung Ah Kang[1], Yea Seong Ryu[1], Xia Han[1], Min Chang Oh[1], Uhee Jung[2], In Gyu Kim[3,4] and Jin Won Hyun[1,*]

[1]School of Medicine, Jeju National University, Jeju 63243, [2]Radiation Biotechnology Research Division, Korea Atomic Energy Research Institute, Jeongeup 56212, [3]Department of Radiation Biology, Environmental Radiation Research Group, Korea Atomic Energy Research Institute, Daejeon 34057, [4]Department of Radiation Biotechnology and Applied Radioisotope, Korea University of Science and Technology, Daejeon 34113, Republic of Korea

Abstract

Human skin cells undergo pathophysiological processes via generation of reactive oxygen species (ROS) upon excessive exposure to ultraviolet B (UVB) radiation. This study investigated the ability of hesperidin ($C_{28}H_{34}O_{15}$) to prevent apoptosis due to oxidative stress generated through UVB-induced ROS. Hesperidin significantly scavenged ROS generated by UVB radiation, attenuated the oxidation of cellular macromolecules, established mitochondrial membrane polarization, and prevented the release of cytochrome c into the cytosol. Hesperidin downregulated expression of caspase-9, caspase-3, and Bcl-2-associated X protein, and upregulated expression of B-cell lymphoma 2. Hesperidin absorbed wavelengths of light within the UVB range. In summary, hesperidin shielded human keratinocytes from UVB radiation-induced damage and apoptosis via its antioxidant and UVB absorption properties.

Key Words: Apoptosis, Antioxidant, Hesperidin, Reactive oxygen species, Ultraviolet B

INTRODUCTION

Skin is the outermost covering of the body and various extrinsic factors affect skin health and cause aging. Ultraviolet radiation (UVR) is one of the main causes of premature skin aging and photo-aging, whereas natural aging is called intrinsic aging (Gilchrest and Yaar, 1992). Although the UVR spectrum is composed of ultraviolet A (UVA, 320-400 nm), ultraviolet B (UVB, 280-320 nm), and ultraviolet C (UVC, <280 nm) based on their wavelengths (Mabruk *et al.*, 2009), almost all UVC radiation and a large portion of UVB radiation are absorbed by the ozone in the stratosphere, making UVA the predominant form of UVR that reaches the earth (Black *et al.*, 1997). However, with the depletion of the ozone layer due to the emission of greenhouse gasses an excessive amount of UVB reaches the earth's surface (Bolaji and Huan, 2013). UVB exposure causes several skin disorders including carcinogenesis, inflammation, solar erythema, and premature aging (Karol, 2009). UVB exposure causes cells to undergo apoptosis by directly or indirectly causing DNA damage (Ravanat *et al.*,

2001). UVA has less energy than UVB. Consequently, UVA can only damage DNA indirectly via the generation of reactive oxygen species (ROS), whereas UVB can damage cells indirectly via the generation of ROS and directly via the formation of pyrimidine dimers and double-strand DNA breaks (Svobodova *et al.*, 2012). ROS (singlet oxygen, superoxide anion, hydroxyl radical, and hydrogen peroxide) generated by UVB not only attack DNA but also cellular macromolecules such as proteins and lipids, and this interrupts cellular metabolism and ultimately leads to apoptosis (Dhumrongvaraporn and Chanvorachote, 2013).

Cellular metabolism also contributes to the formation of ROS; in particular, all mammalian aerobic cells generate considerable amounts of ROS via the electron transport chain at the inner mitochondrial membrane (Turrens, 2003). However, the antioxidant defense system, which comprises enzymes such as catalase, superoxide dismutase, and glutathione peroxidase as well as antioxidants such as α-tocopherol and carotenoids, maintains ROS at optimal levels (Shindo *et al.*, 1994). External sources of ROS, such as UVB, can over-

www.biomolther.org

whelm this equilibrium and cells are subsequently exposed to oxidative stress, which causes the aforementioned negative effects and ultimately apoptosis (Waster and Ollinger, 2009). Many efforts have sought to overcome the adverse effects of UVR exposure. Biological compounds with antioxidant properties, especially phytochemicals, protect cells and tissues against the deleterious effects of ROS and other free radicals (Campanini et al., 2013).

Hesperidin (hesperetin 7-rutinoside) is a flavanone glycoside that is abundant in citrus fruits. Hesperidin reduces blood pressure (Ohtsuki et al., 2003) and the cholesterol level (Chiba et al., 2003) in rats. Furthermore, hesperidin has a wide range of biological effects, from anticancer and antibacterial activities to inhibition of bone reabsorption and neuroprotective effects (Amado et al., 2009). However, little is known about the effect of hesperidin on UVB-induced skin cell damage. The present study investigated the mechanisms underlying the protective effects of hesperidin against UVB-induced oxidative damage in human keratinocytes.

MATERIALS AND METHODS

Reagents

Hesperidin ($C_{28}H_{34}O_{15}$), 1,1-diphenyl-2-picrylhydrazyl (DPPH) radical, N-acetylcysteine (NAC), 5,5-dimethyl-1-pyrroline-N-oxide (DMPO), 2',7'-dichlorodihydrofluorescein diacetate (DCF-DA), 3-(4,5-dimethylthiazol-2-yl)-2,5-diphenyltetrazolium bromide (MTT), Hoechst 33342 dye and primary antibody against actin were purchased from Sigma-Aldrich Inc. (St. Louis, MO, USA). 5,5',6,6'-Tetrachloro-1,1',3,3'-tetraethyl-benzimidazolylcarbocyanine iodide (JC-1) was purchased from Invitrogen (Carlsbad, CA, USA). Primary antibodies against Bcl-2-associated X protein (BAX) and B-cell lymphoma 2 (Bcl-2) were purchased from Santa Cruz Biotechnology Inc. (Dallas, TX, USA). Primary antibodies against caspase-3 and caspase-9 were purchased from Cell Signaling Technology (Danvers, MA, USA). All other chemicals and reagents were of analytical grade.

Cell culture and UVB exposure

The human keratinocyte cell line HaCaT was purchased from Amore Pacific Company (Yongin, Republic of Korea) and cells were maintained at 37ºC in an incubator with a humidified atmosphere of 5% CO_2. Cells were cultured in RPMI 1640 medium containing 10% heat-inactivated fetal bovine serum, streptomycin (100 μg/ml), and penicillin (100 units/ml). Cells were exposed to UVB at a dose of 30 mJ/cm^2. The CL-1000M UV Crosslinker (UVP, Upland, CA, USA) was used as the UVB source and delivered a UVB energy spectrum of 280-320 nm.

Detection of DPPH radicals

The ability of hesperidin to scavenge DPPH radicals was assessed. Hesperidin (12.5, 25, 50, or 100 μM) or 1 mM NAC was added to a 96-well plate. DPPH dissolved in ethanol (0.1 mM) was added to each well up to a volume of 200 μl. After shaking for 3 h, unreacted DPPH was detected by measuring absorbance at 520 nm using a spectrophotometer.

Detection of intracellular ROS

The DCF-DA fluorescence detection method was used to measure intracellular ROS generated by H_2O_2 or UVB (Rosenkranz et al., 1992). Cells were seeded at a density of 1.5×10^5 cells/ml and incubated at 37ºC for 24 h. Hesperidin or NAC (1 mM) was added to each well. After 0.5-1 h, cells were treated with H_2O_2 (1 mM) or exposed to UVB. After 30 min, H_2O_2-treated cells were treated with DCF-DA (25 μM) and incubated for another 20 min. UVB-treated cells were incubated for 24 h, after which DCF-DA (50 μM) was added and cells were incubated for a further 2 h. The fluorescence of 2',7'-dichlorofluorescein was detected and quantified using a PerkinElmer LS-5B spectrofluorometer (PerkinElmer, Waltham, MA, USA).

Cell viability assay

The effect of hesperidin on cell viability was examined using the MTT assay. Cells were seeded in a 96-well plate at a density of 1×10^5 cells/ml. After 24 h, hesperidin was added to a final concentration of 12.5, 25, 50, or 100 μM and cells were incubated for a further 24 h. In UVB group, cells were exposed to UVB (30 mJ/cm^2) at 1 h after the hesperidin treatment and incubated for a further 24 h. MTT stock solution (50 μl, 2 mg/ml) was added to each well to yield a final reaction volume of 200 μl. The supernatant was aspirated 4 h later and formazan crystals were dissolved in 150 μl of dimethylsulfoxide (DMSO). The absorbance at 540 nm was measured using a scanning multi-well spectrophotometer.

Detection of hydroxyl radicals

Hydroxyl radicals generated by the Fenton reaction (H_2O_2+ $FeSO_4$) were reacted with DMPO. The resultant DMPO/•OH adducts were detected using an electron spin resonance (ESR) spectrometer (Li et al., 2003). The ESR spectrum was recorded 2.5 min after phosphate buffer (pH 7.4) was mixed with 0.02 ml each of 0.3 M DMPO, 10 mM $FeSO_4$, 10 mM H_2O_2, and 50 μM hesperidin. The ESR spectrometer parameters were set as follows: central magnetic field, 336.8 mT; power, 1.00 mW; frequency, 9.4380 GHz; modulation width, 0.2 mT; amplitude, 600; sweep width, 10 mT; sweep time, 0.5 min; time constant, 0.03 sec; temperature, 25ºC.

Ultraviolet (UV)/visible light absorption analysis

Absorption analysis of hesperidin (50 μM) was performed by scanning with UV/visible light of a wavelength of 200-400 nm using an HP-8453E UV-visible spectroscopy system (Hewlett Packard, Palo Alto, CA, USA) and a standard quartz cuvette with a 1 cm path length. Hesperidin was diluted in 1× phosphate-buffered saline (PBS) to a final concentration of 50 μM prior to scanning.

Single cell gel electrophoresis (comet assay)

DNA damage caused by oxidative stress was detected using the comet assay (Singh, 2000). Cells were seeded at a density of 1×10^5 cells/ml and then treated with hesperidin (50 μM) and exposed to UVB (30 mJ/cm^2) 30 min later. The cell suspension was collected and mixed with 120 μl of 0.7% low melting agarose (LMA) at 37ºC. The mixture was spread on a fully frosted microscopy slide pre-coated with 200 μl of 1% normal melting agarose. After the LMA had solidified, another 170 μl of LMA was spread over the slide. Slides were immersed in lysis solution (2.5 M NaCl, 100 mM Na-EDTA, 10 mM Tris, 1% Trion X-100, and 10% DMSO, pH 10) for 90 min at 4ºC. Slides were then immersed in unwinding buffer (300 mM NaOH and 10 mM Na-EDTA, pH 13) for 30 min at 4ºC. Slides were subjected to electrophoresis in unwinding buffer with an electrical field of 300 mA (constant) and 25 V for
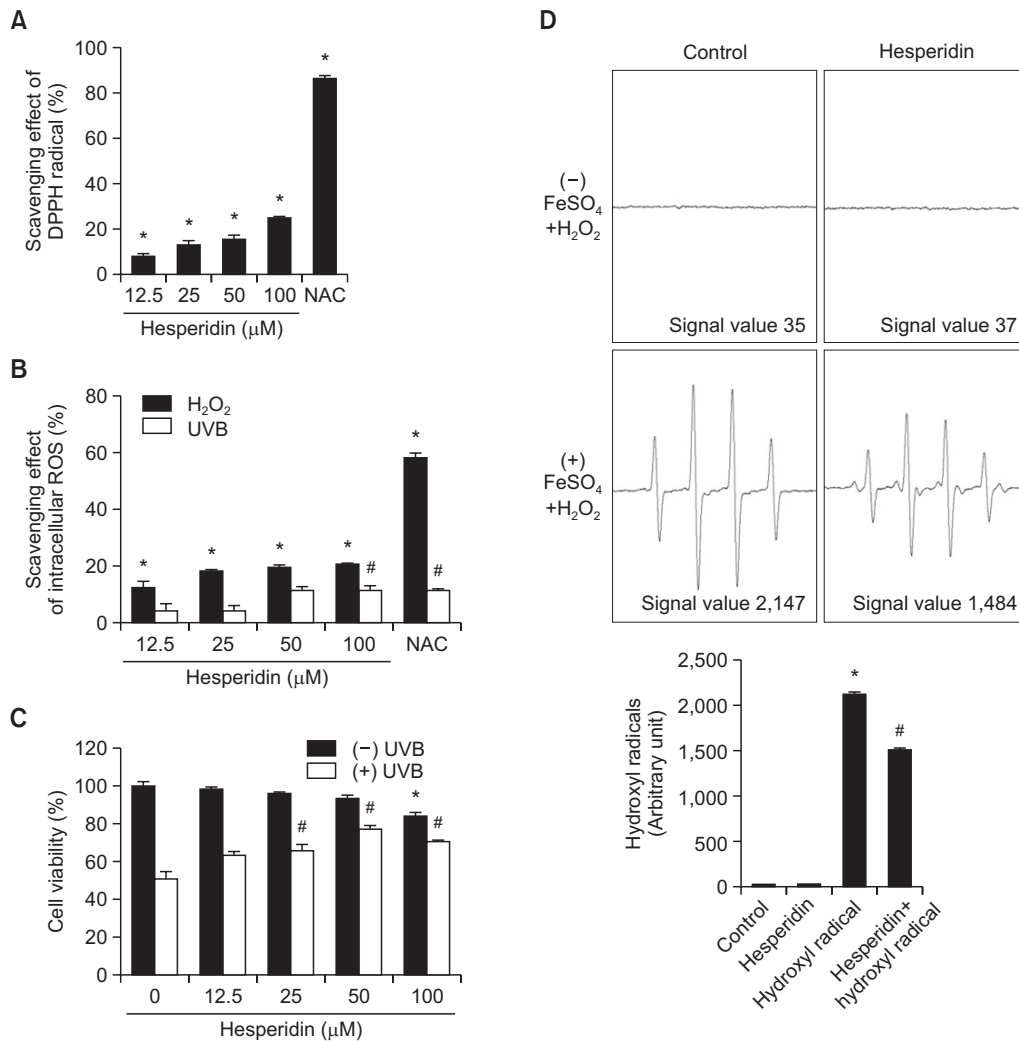
Fig. 1. Hesperidin scavenges the DPPH radical and intracellular ROS, and protects against cell death induced by UVB. (A) Various concentrations of hesperidin were added to DPPH and the level of remaining DPPH radicals was determined by measuring absorbance at 520 nm using a spectrophotometer. NAC was used as the positive control. *Significantly different from the control ($p<0.05$). (B) Cells were treated with various concentrations of hesperidin for 1 h, treated with 1 mM H_2O_2 or irradiated with 30 mJ/cm^2 UVB, and incubated for a further 24 h. Intracellular ROS were detected by DCF-DA staining using fluorescence spectrophotometry. NAC was used as the positive control. *,#Significantly different from control H_2O_2-treated or UVB-irradiated cells, respectively ($p<0.05$). (C) Cell viability following treatment with various concentrations of hesperidin was determined using the MTT assay. *,#Significantly different from control and UVB-irradiated cells, respectively ($p<0.05$). (D) The hydroxyl radical generated by the Fenton reaction (H_2O_2+FeSO$_4$) was reacted with DMPO and the resulting DMPO/·OH adducts were detected by ESR spectrometry. Results are expressed as representative peak data and a representative histogram is shown. *,#Significantly different from the control and hydroxyl radicals generated by the Fenton reaction in the absence of hesperidin, respectively ($p<0.05$).

20 min at room temperature. Slides were washed three times with neutralizing buffer (0.4 M Tris, pH 7.5) for 10 min each time and then washed with 70% ethanol for 5 min. Slides were stained with 70 μl of ethidium bromide and observed under a fluorescence microscope and image analyzer (Kinetic Imaging, Komet 5.5, UK). The tail length and percentage of fluorescence in the tail were recorded for 50 cells per slide.

DNA fragmentation assay

HaCaT cells were cultured in a 24-well plate at a density of 2×10^5 cells/ml, incubated for 24 h, and then treated with hesperidin (50 μM). One hour later, cells were exposed to UVB and incubated for a further 24 h. DNA fragmentation

was assessed by photometric detection of bromodeoxyuridine (BrdU)-labeled DNA fragments in the culture supernatant. A commercial enzyme-linked immunosorbent assay kit was used according to the manufacturer's instructions (Roche Applied Science, Mannheim, Germany).

8-Isoprostane assay

Cells were treated with hesperidin (50 μM) for 24 h. One hour later, cells were exposed to UVB and incubated at 37°C for another 24 h. Lipid peroxidation was assayed by colorimetric determination of the level of 8-isoprostane secreted into the culture medium by HaCaT keratinocytes (Beauchamp *et al.*, 2002). A commercial enzyme-linked immunosorbent assay

(ELISA) (Cayman Chemical, Ann Arbor, MI, USA) was used according to the manufacturer's instructions.

Protein carbonylation assay

Cells were treated with hesperidin (50 μM). One hour later, cells were exposed to UVB and incubated at 37ºC for another 24 h. The extent of protein carbonyl formation was determined using an Oxiselect™ protein carbonyl ELISA kit from Cell Bio-

Fig. 2. Hesperidin absorbs UVB radiation. The absorption spectrum of hesperidin (50 μM) was measured with UV/visible light of a wavelength of 200-400 nm using an UV-visible spectroscopy system.

labs (San Diego, CA, USA) according to the manufacturer's instructions.

Nuclear staining with Hoechst 33342

Cells were treated with hesperidin (50 μM) and exposed to UVB radiation 3 h later. After incubation for 24 h at 37ºC, the DNA-specific fluorescent dye Hoechst 33342 (1 μl of a 20 mM stock) was added to each well and cells were incubated for 10 min at 37ºC. Stained cells were visualized using a fluorescence microscope equipped with a CoolSNAP-Pro color digital camera. The degree of nuclear condensation was evaluated by counting cells in randomly selected uniform sized areas.

Analysis of mitochondrial membrane potential

Mitochondrial membrane potential was analyzed by flow cytometry. Cells were harvested, washed, suspended in PBS containing JC-1 (10 μg/ml), incubated for 15 min at 37ºC, and analyzed by flow cytometry (Troiano et al., 2007).

Western blot analysis

Harvested cells were lysed by incubation on ice for 10 min in 150 μl of lysis buffer (iNtRON Biotechnology, Republic of Korea). The resultant cell lysates were centrifuged at 13,000 rpm for 5 min. Supernatants were collected and protein concentrations were determined. Aliquots were boiled for 5 min and electrophoresed on 12% SDS-polyacrylamide gels. Protein blots of the gels were transferred to nitrocellulose membranes. The membranes were incubated with the appropriate
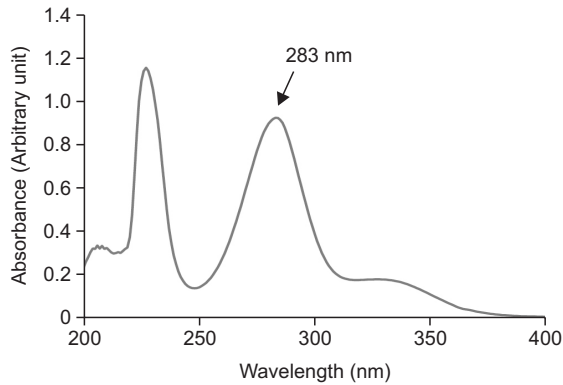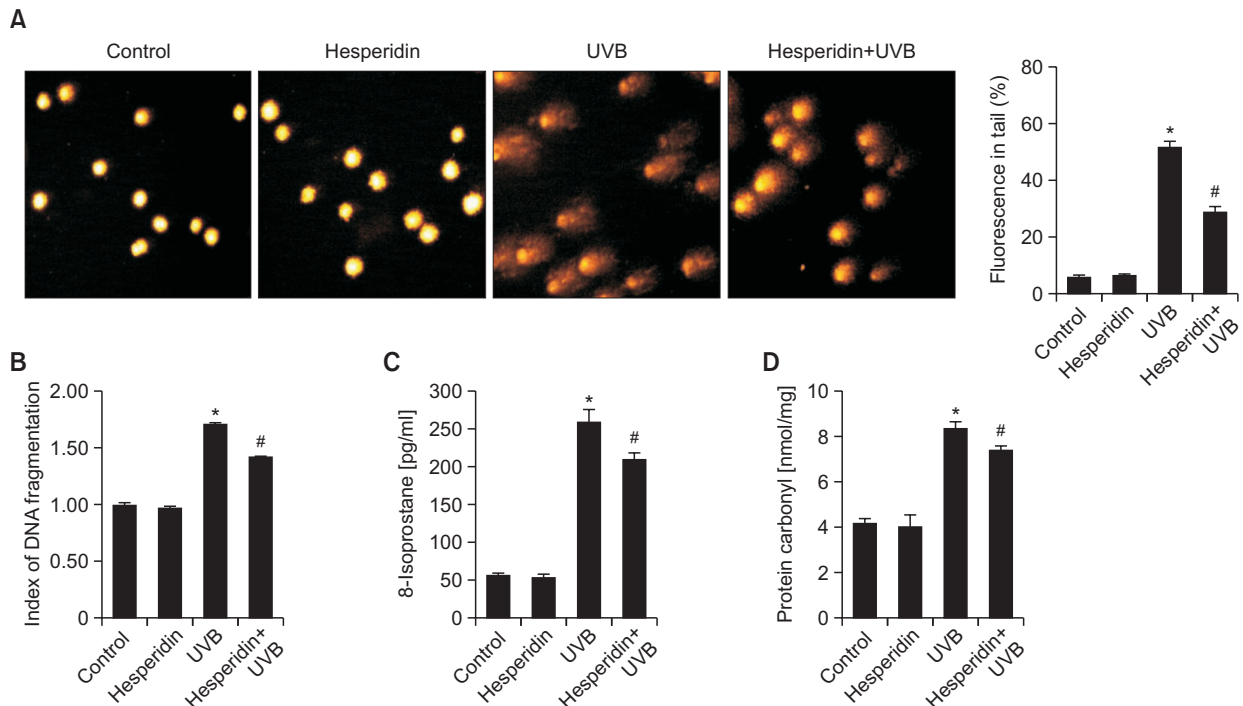

Fig. 3. Hesperidin protects against UVB-induced oxidative damage to cellular macromolecules. HaCaT cells were treated with hesperidin (50 μM) for 1 h and then exposed to UVB radiation. (A) DNA damage was measured by the alkaline comet assay. Representative images and the percentage of total DNA fluorescence in comet tails are shown. (B) After 24 h of incubation, DNA fragmentation was assessed by colorimetric determination of BrdU-labeled DNA fragments. (C) Lipid peroxidation was measured by detecting the level of 8-isoprostane secreted into the culture medium. (D) Protein oxidation was assayed by detecting the level of protein carbonyls. *,#Significantly different from control and UVB-irradiated cells, respectively ($p < 0.05$).

primary antibodies (1:1,000) followed by horseradish perox-idase-conjugated anti-IgG secondary antibodies (1:5,000) (Pierce, Rockford, IL, USA). Protein bands were detected using an Enhanced Chemiluminescence Western Blotting Detection Kit (Amersham, Little Chalfont, Buckinghamshire, UK).

Statistical analysis

All measurements were performed in triplicate and all values are expressed as means ± standard error. The results were subjected to an analysis of variance using Tukey's test to analyze differences between means. In each case, a *p* value of <0.05 was considered statistically significant.

RESULTS

Scavenging effect of hesperidin against UVB-induced ROS

To confirm the antioxidant properties of hesperidin, DPPH scavenging was first examined. Hesperidin showed promising scavenging of the DPPH radical in a concentration-dependent manner (Fig. 1A). The ability of hesperidin to scavenge intracellular ROS following H_2O_2 treatment or UVB exposure was measured using DCF-DA (Fig. 1B). For all these assays, NAC was used as a positive control. The ability of hesperidin to protect cells after exposure to UVB was determined using the MTT assay (Fig. 1C). More than 76% of cells survived when pretreated with 50 μM hesperidin prior to UVB exposure. However, this protective effect was significantly reduced at concentrations higher than 50 μM. Considering the DPPH and intracellular ROS scavenging activities of hesperidin and the cell viability data, the optimal hesperidin concentration was determined to be 50 μM. This concentration was used in all subsequent experiments. ESR spectrometry was performed to assess the ability of hesperidin (50 μM) to scavenge hydroxyl radicals. In the Fenton reaction ($Fe^{2+}+H_2O_2 \rightarrow Fe^{3+}+\cdot OH +OH^-$), DMPO/·OH adducts generated a signal of 2,147 in the absence of hesperidin and this was reduced to 1,484 in the presence of hesperidin (Fig. 1D).

Ability of hesperidin to absorb UVB

To determine whether hesperidin itself absorbs UVB, its absorption spectrum from 200 nm to 400 nm was investigated. The absorbance profile of hesperidin exhibited two prominent peaks at 227 nm and 283 nm (Fig. 2). Since UVB lays wavelength between 280 and 320 nm; it confirms that hesperidin itself can absorb UVB radiation.

Protective effects of hesperidin against UVB-induced damage to cellular macromolecules

When the ROS level exceeds the capacity of the antioxidant defense system, ROS initiate chain reactions by oxidizing cellular macromolecules, causing the cells to malfunction and eventually undergo programmed cell death (Cross *et al.*, 1987). Visualization of the DNA tail length in microscopy images illustrates DNA strand-breaks. Therefore, the comet assay was performed to assay DNA damage caused by UVB. The percentage of fluorescence in the comet tail was reduced from 51% in cells only exposed to UVB to 28% in cells exposed to UVB and pretreated with hesperidin (Fig. 3A). To confirm the comet assay results, DNA fragmentation assay was performed. BrdU-labeled DNA fragments were photometrically detected in the cell culture supernatant. As expected,

UVB exposure yielded a higher DNA fragmentation index than the control, and hesperidin pretreatment significantly reduced this index (Fig. 3B). The oxidized lipid content was measured by detecting 8-isoprostane, which is a by-product of ROS-induced lipid peroxidation and is used as a specific index of cellular lipid peroxidation (Belli *et al.*, 2005). UVB exposure significantly increased the 8-isoprostane concentration in the culture supernatant of HaCaT cells to 258 pg/ml compared with the control, whereas this was reduced to 210 pg/ml by pretreatment with hesperidin, indicative of a reduced level of lipid peroxidation in hesperidin-treated cells (Fig. 3C). Proteins are an important target of ROS in cells. Protein carbonylation is a biomarker of cellular damage following oxidative stress (Dalle-Donne *et al.*, 2003). Protein oxidization was investigated by determining the level of protein carbonylation. The concentration of protein carbonyls was higher in UVB-exposed cells (8.3 nmol/mg) than in control cells. However, hesperidin pretreatment significantly reduced the level of protein carbonylation (7.3 nmol/mg) in UVB-exposed keratinocytes (Fig. 3D). These results revealed that pretreatment with hesperidin significantly attenuated cellular macromolecule damage caused by UVB-induced oxidative stress.

Effects of hesperidin on UVB-induced apoptosis

MTT assay showed that hesperidin increased the viability of UVB-exposed cells (Fig. 1C). We examined whether hesperidin attenuated apoptosis in HaCaT cells by staining the cells with Hoechst 33342 and performing fluorescence microscopy. NAC was used as a positive control. Clear nuclear fragmentation was observed in UVB-irradiated cells (apoptotic index, 41), whereas hesperidin pretreatment dramatically reduced nuclear fragmentation (apoptotic index, 10) (Fig. 4A). Depolarization of the inner mitochondrial membrane causes the release of cytochrome c into the cytosol, where it activates the intrinsic apoptotic pathway via triggering caspase protein cascades (Li *et al.*, 1997). Therefore, mitochondrial depolarization was investigated by flow cytometric analysis of cells stained with JC-1 staining dye. The fluorescence intensity of JC-1 was markedly higher in UVB-exposed cells than in control cells, but was markedly reduced in cells pretreated with hesperidin prior to UVB exposure, indicating that hesperidin can establish mitochondrial polarization and prevent the release of cytochrome c into the cytosol (Fig. 4B). Caspase proteins, which belong to the family of cysteine proteases, play an essential role in apoptosis (Wilson *et al.*, 1994). The mitochondrial release of cytochrome c activates pro-caspase-9, after which activated caspase-9 propagates a caspase cascade to activate other caspases, resulting in the activation of caspase-3 and the induction of apoptosis (Adrain and Martin, 2001). Therefore, caspase-9 and caspase-3 protein expression was examined by western blot analysis. Levels of cleaved caspase-9 and cleaved caspase-3 were markedly lower in cells pretreated with hesperidin and exposed to UVB than in cells only exposed to UVB (Fig. 4C). Bcl-2 and BAX have opposite functions in apoptosis; the former is anti-apoptotic, whereas the latter is pro-apoptotic (Antonsson *et al.*, 1997). Hesperidin pretreatment markedly upregulated expression of Bcl-2 and notably downregulated expression of BAX in UVB-irradiated cells (Fig. 4C). These findings suggest that hesperidin interrupts caspase cascades activated by UVB-induced oxidative damage and enhances cell survival.
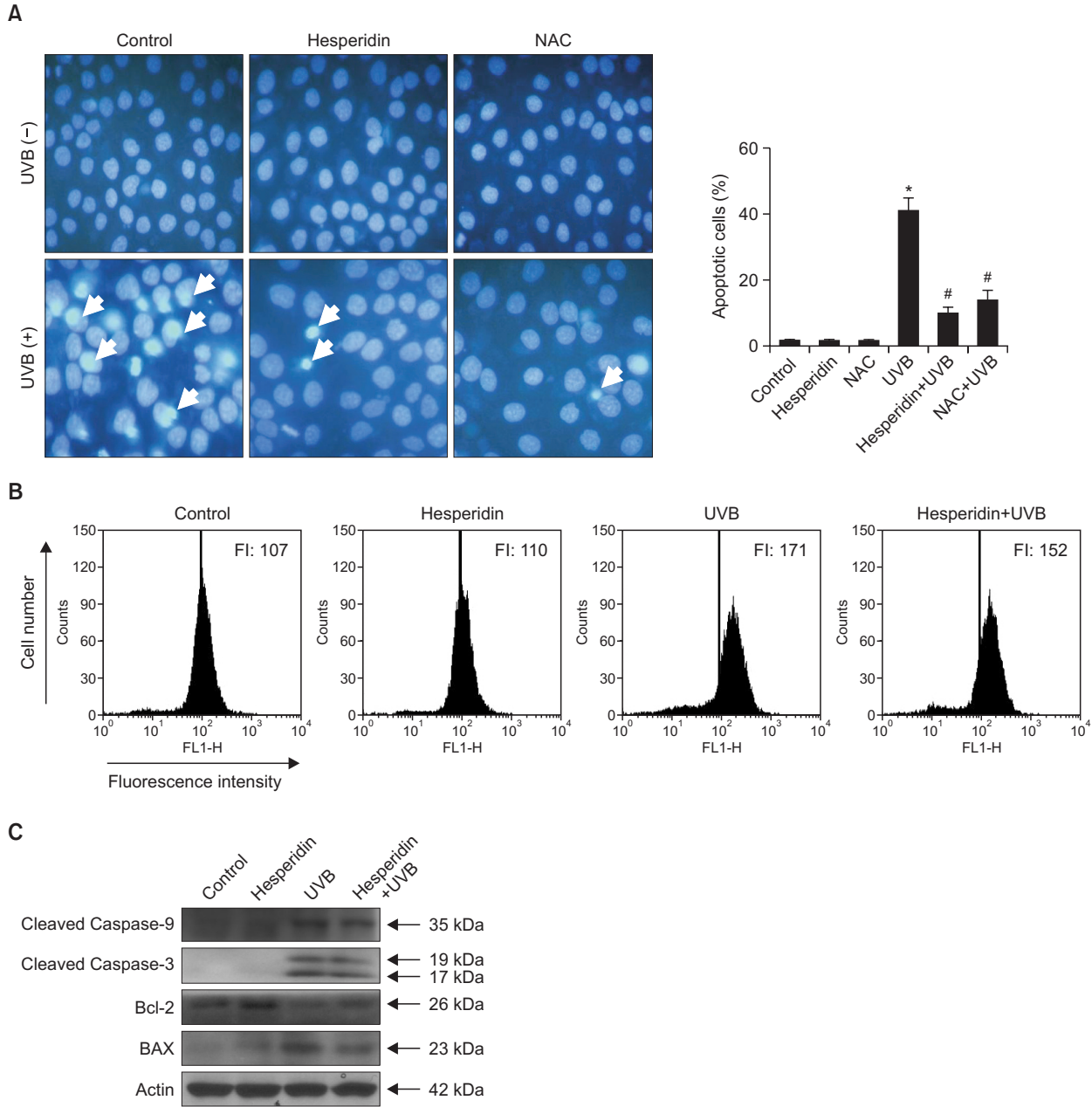
A

B

C

Fig. 4. Hesperidin suppresses UVB-induced apoptosis via preventing disruption of the mitochondrial membrane potential and the activation of caspase cascades. Cells were pretreated with 50 μM hesperidin and irradiated with 30 mJ/cm^2 UVB after 1 h. (A) Formation of apoptotic bodies was observed under a fluorescence microscope following Hoechst 33342 staining. The ratio between apoptotic bodies (arrows) and the total number of cells was determined within a randomly selected area (0.3 mm^2) of each well. Apoptotic bodies are indicated by arrows. *,#Significantly different from control and UVB-irradiated cells, respectively ($p<0.05$). NAC was used as the positive control. (B) Cells were stained with JC-1 and mitochondrial membrane potential was analyzed by flow cytometry. (C) Cleaved caspase-9, cleaved caspase-3, Bcl-2, and BAX were detected using specific antibodies.

DISCUSSION

The intensity of UVB radiation that reaches the earth has dramatically increased due to the depletion of the ozone layer (McKenzie et al., 2011). Although UVB has beneficial functions for humans, such as in vitamin D synthesis, excessive exposure to UVB radiation causes cell damage, cell death, and skin cancer (Drouin and Therrien 1997). These undesirable effects of UVB are mainly owing to the generation of ROS and DNA damage (Ravanat et al., 2001). This study focused on the antioxidant effects of hesperidin to attenuate UVB-induced oxidative damage and apoptosis in human keratinocytes. Hesperidin scavenged DPPH radicals (Fig. 1A) and intracellular ROS generated by H$_2$O$_2$ treatment and UVB irradiation in a dose-dependent manner (Fig. 1B). Of the various concentrations tested, 50 μM was selected as the optimal concentration

of hesperidin for further analysis because it yielded the highest cell viability and scavenging activities (Fig. 1C). ESR results confirmed that hesperidin scavenged hydroxyl radicals generated through the Fenton reaction in cell-free systems (Fig. 1D). These data show that hesperidin has antioxidant property that protects cells against UVB-induced oxidative stress. The absorption spectrum of hesperidin showed a large peak at 283 nm, revealing that, in addition to scavenging ROS, hesperidin can absorb UVB radiation (Fig. 2).

When the antioxidant defense system is overwhelmed by increased ROS production, ROS will cause DNA single and double-strand breaks, induce DNA-protein cross-linking (Caldwell *et al*., 2007), and attack other important cellular macromolecules such as lipids and proteins, thereby interrupting cellular activities and ultimately causing apoptosis (Dhumrongvaraporn and Chanvorachote, 2013). UVB exposure dramatically increased the levels of DNA damage and membrane lipid peroxidation. The comet assay, the DNA fragmentation assay, and detection of 8-isoprostane, which is a stable indicator of lipid peroxidation, revealed that hesperidin attenuated this damage (Fig. 3A-C). Oxidation of amino acids such as lysine, arginine, and proline in response to oxidative stress results in the formation of carbonyl derivatives, which perturbs the functions of cellular proteins (Levine *et al*., 1990). Hesperidin prevented the oxidation of proteins by UVB-induced ROS (Fig. 3D).

Hoechst 33342 staining elucidated the anti-apoptotic effects of hesperidin (Fig. 4A). As a result of oxidative stress, the depolarized inner mitochondrial membrane allows the release of cytochrome c into the cytosol, which triggers caspase cascades and initiates the intrinsic apoptotic pathway (Arends *et al*., 1990). Hesperidin restored mitochondrial membrane depolarization, thereby preventing the release of cytochrome c (Fig. 4B). Cytochrome c, deoxyadenosine triphosphate, and apoptotic protease-activating factor 1, which are key components of the apoptosome, activate caspase-9. This leads to the activation of downstream caspases (Slee *et al*., 1999), including caspase-3, which cleave inhibitor of caspase-activated DNase, resulting in DNA degradation or fragmentation (Enari *et al*., 1998). The mitochondria-mediated apoptotic pathway is largely controlled by Bcl-2 family proteins such as the pro-apoptotic proteins BAX, Bak, and BNIP3, which promote mitochondrial permeability, and the anti-apoptotic proteins Bcl-2 and Bcl-xL, which restore mitochondrial polarization (Antonsson *et al*., 1997). Hesperidin downregulated expression of caspase-3, caspase-9, and BAX, and upregulated expression of Bcl-2 (Fig. 4C). Some studies have reported that hesperidin significantly induced apoptosis by modulating BAX/Bcl-2 ratio together with enhanced cytochrome c release and caspase activations in colon cancer cells (Saiprasad *et al*., 2014) and mediates apoptosis though extrinsic pathway in cervical cancer cells (Bartoszewski *et al*., 2014). Excessive ROS triggers oxidative stress in cancer microenvironment and leads to stimulation of various oxidative stress-induced oncogenic signaling molecules (Zhang *et al*., 2008). It has been reported that an antioxidant compound, quercetin, exhibits anticancer effect through the upregulation of p53 and BAX via downregulation of ROS, protein kinase C and, phosphatidylinositol 3-kinase in HepG2 cells (Maurya and Vinayak 2015). Therefore along with these findings, antioxidant effect of hesperidin might lead to show the anticancer effects in various cancer cells.

In summary, this study showed that hesperidin protects hu-

man skin keratinocytes against UVB-induced oxidative stress by scavenging ROS, absorbing UVB radiation, establishing mitochondrial polarity, and regulating apoptotic proteins.

REFERENCES

Adrain, C. and Martin, S. J. (2001) The mitochondrial apoptosome: A killer unleashed by the cytochrome seas. *Trends Biochem. Sci.* **26**, 390-397.

Amado, N. G., Cerqueira, D. M. and Menezes, F. S. (2009) Isoquercitrin isolated from Hyptis fasciculata reduces glioblastoma cell proliferation and changes beta-catenin cellular localization. *Anticancer Drugs* **20**, 543-552.

Antonsson, B., Conti, F., Ciavatta, A., Montessuit, S., Lewis, S., Martinou, I., Bernasconi, L., Bernard, A., Mermod, J. J., Mazzei, G., Maundrell, K., Gambale, F., Sadoul, R. and Martinou, J. C. (1997) Inhibition of Bax channel-forming activity by Bcl-2. *Science* **277**, 370-372.

Arends, M. J., Morris, R. G. and Wyllie, A. H. (1990) Apoptosis. The role of the endonuclease. *Am. J. Pathol.* **136**, 593-608.

Bartoszewski, R., Hering, A., Marszałł, M., Stefanowicz Hajduk, J., Bartoszewska, S., Kapoor, N., Kochan, K. and Ochocka, R. (2014) Mangiferin has an additive effect on the apoptotic properties of hesperidin in Cyclopia sp. tea extracts. *PLoS One.* **3**, e92128.

Beauchamp, M. C., Letendre, E. and Renier, G. (2002) Macrophage lipoprotein lipase expression is increased in patients with heterozygous familial hypercholesterolemia. *J. Lipid Res.* **43**, 215-222.

Belli, R., Amerio, P., Brunetti, L., Orlando, G., Toto, P., Proietto, G., Vacca, M. and Tulli, A. (2005) Elevated 8-isoprostane levels in basal cell carcinoma and in UVA irradiated skin. *Int. J. Immunopathol. Pharmacol.* **18**, 497-502.

Black, H. S., de Gruijl, F. R., Forbes, P. D., Cleaver, J. E., Ananthaswamy, H. N., de Fabo, E. C., Ullrich, S. E. and Tyrrell, R. M. (1997) Photocarcinogenesis: an overview. *J. Photochem. Photobiol. B* **40**, 29-47.

Bolaji, B. and Huan, Z. (2013) Ozone depletion and global warming: Case for the use of natural refrigerant-a review. *Renew. Sustain. Energy Rev.* **18**, 49-54.

Caldwell, M. M., Bornman, J. F., Ballare, C. L., Flint, S. D. and Kulandaivelu, G. (2007) Terrestrial ecosystems, increased solar ultraviolet radiation and interactions with other climate change factors. *Photochem. Photobiol. Sci.* **6**, 252-266.

Campanini, M. Z., Pinho-Ribeiro, F. A., Ivan, A. L., Ferreira, V. S., Vilela, F. M., Vicentini, F. T., Martinez, R. M., Zarpelon, A. C., Fonseca, M. J., Faria, T. J., Baracat, M. M., Verri, W. A., Georgetti, S. R. and Casagrande, R. (2013) Efficacy of topical formulations containing Pimenta pseudocaryophyllusextract against UVB-induced oxidative stress and inflammation in hairless mice. *J. Photochem. Photobiol. B* **127**, 153-160.

Chiba, H., Uehara, M., Wu, J., Wang, X., Masuyama, R., Suzuki, K., Kanazawa, K. and Ishimi, Y. (2003) Hesperidin, a citrus flavonoid, inhibits bone loss and decreases serum and hepatic lipids in ovariectomized mice. *J. Nutr.* **133**, 1892-1897.

Cross, C. E., Halliwell, B., Borish, E. T., Pryor, W. A., Ames, B. N., Saul, R .L., McCord, J. M. and Harman, D. (1987) Oxygen radicals and human disease. *Ann. Intern. Med.* **107**, 526-545.

Dalle-Donne, I., Rossi, R., Giustarini, D., Milzani, A. and Colombo, R. (2003) Protein carbonyl groups as biomarkers of oxidative stress. *Clin. Chim. Acta* **329**, 23-38.

Dhumrongvaraporn, A. and Chanvorachote, P. (2013) Kinetics of ultraviolet B irradiation-mediated reactive oxygen species generation in human keratinocytes. *J. Cosmet. Sci.* **64**, 207-217.

Drouin, R. and Therrien, J. P. (1997) UVB-induced cyclobutane pyrimidine dimer frequency correlates with skin cancer mutational hotspots in p53. *Photochem. Photobiol.* **66**, 719-726.

Enari, M., Sakahira, H., Yokoyama, H., Okawa, K., Iwamatsu, A. and Nagata, S. (1998) A caspase-activated DNase that degrades DNA during apoptosis, and its inhibitor ICAD. *Nature* **391**, 43-50.

Gilchrest, B. A. and Yaar, M. (1992) Ageing and photoageing of the skin: observations at the cellular and molecular level. *Br. J. Dermatol.* **127**, 25-30.

Karol, M. H. (2009) How environmental agents influence the aging process. *Biomol. Ther. (Seoul)* **17**, 113-124.

Levine, R. L., Garland, D., Oliver, C. N., Amici, A., Climent, I., Lenz, A. G., Ahn, B. W., Shaltiel, S. and Stadtman, E. R. (1990) Determination of carbonyl content in oxidatively modified proteins. *Methods Enzymol.* **186**, 464-478.

Li, L, Abe, Y., Mashino, T., Mochizuki, M. and Miyata, N. (2003) Signal enhancement in ESR spin-trapping for hydroxyl radicals. *Anal. Sci.* **19**, 1083-1084.

Li, P., Nijhawan, D., Budihardjo, I., Srinivasula, S. M., Ahmad, M., Alnemri, E. S. and Wang, X. (1997) Cytochrome c and dATP-dependent formation of Apaf-1/caspase-9 complex initiates an apoptotic protease cascade. *Cell* **91**, 479-489.

Mabruk, M. J., Toh, L. K., Murphy, M., Leader, M., Kay, E. and Murphy, G. M. (2009) Investigation of the effect of UV irradiation on DNA damage: comparison between skin cancer patients and normal volunteers. *J. Cutan. Pathol.* **36**, 760-765.

Maurya, A. K. and Vinayak, M. (2015) Anticarcinogenic action of quercetin by downregulation of phosphatidylinositol 3-kinase (PI3K) and protein kinase C (PKC) via induction of p53 in hepatocellular carcinoma (HepG2) cell line. *Mol. Biol. Rep.* **42**, 1419-1429.

McKenzie, R. L., Aucamp, P. J., Bais, A. F., Bjorn, L. O., Ilyas, M. and Madronich, S. (2011) Ozone depletion and climate change: impacts on UV radiation. *Photochem. Photobiol. Sci.* **10**, 182-198.

Ohtsuki, K., Abe, A., Mitsuzumi, H., Kondo, M., Uemura, K., Iwasaki, Y. and Kondo, Y. (2003). Glucosyl hesperidin improves serum cholesterol composition and inhibits hypertrophy in vasculature. *J. Nutr. Sci. Vitaminol.* **49**, 447-450.

Ravanat, J. L., Douki, T. and Cadet, J. (2001) Direct and indirect effects of UV radiation on DNA and its components. *J. Photochem. Photobiol. B* **63**, 88-102.

Rosenkranz, A. R., Schmaldienst, S., Stuhlmeier, K. M., Chen, W., Knapp, W. and Zlabinger, G. J. (1992) A microplate assay for the detection of oxidative products using 2',7' dichlorofluorescin-diacetate. *J. Immunol. Methods* **156**, 39-45.

Saiprasad, G., Chitra, P., Manikandan, R. and Sudhandiran, G. (2014) Hesperidin induces apoptosis and triggers autophagic markers through inhibition of Aurora-A mediated phosphoinositide-3-kinase/Akt/mammalian target of rapamycin and glycogen synthase kinase-3 beta signalling cascades in experimental colon carcinogenesis. *Eur. J. Cancer* **50**, 2489-2507.

Shindo, Y., Witt, E., Han, D., Epstein, W. and Packer, L. (1994) Enzymic and non-enzymic antioxidants in epidermis and dermis of human skin. *J. Invest. Dermatol.* **102**, 122-124.

Singh, N. P. (2000) Microgels for estimation of DNA strand breaks, DNA protein crosslinks and apoptosis. *Mutat. Res.* **455**, 111-127.

Slee, E. A., Harte, M. T., Kluck, R. M., Wolf, B. B., Casiano, C. A., Newmeyer, D. D., Wang, H. G., Reed, J. C., Nicholson, D. W., Alnemri, E. S., Green, D. R. and Martin, S. J. (1999) Ordering the cytochrome c-initiated caspase cascade: hierarchical activation of caspases-2, -3, -6, -7, -8, and -10 in a caspase-9-dependent manner. *J. Cell Biol.* **144**, 281-292.

Svobodova, A. R., Galandakova, A., Sianska, J., Dolezal, D., Lichnovska, R., Ulrichova, J. and Vostalova, J. (2012) DNA damage after acute exposure of mice skin to physiological doses of UVB and UVA light. *Arch. Dermatol. Res.* **304**, 407-412.

Troiano, L., Ferraresi, R., Lugli, E., Nemes, E., Roat, E., Nasi, M., Pinti, M. and Cossarizza, A. (2007) Multiparametric analysis of cells with different mitochondrial membrane potential during apoptosis by polychromatic flow cytometry. *Nat. Protoc.* **2**, 2719-2727.

Turrens, J. F. (2003) Mitochondrial formation of reactive oxygen species. *J. Physiol.* **552**, 335-344.

Waster, P. K. and Ollinger, K. M. (2009) Redox-dependent translocation of p53 to mitochondria or nucleus in human melanocytes after UVA- and UVB-induced apoptosis. *J. Invest. Dermatol.* **129**, 1769-1781.

Wilson, K. P., Black, J. A., Thomson, J. A., Kim, E. E., Griffith, J. P., Navia, M. A., Murcko, M. A., Chambers, S. P., Aldape, R. A., Raybuck, S. A. and David, J. L. (1994) Structure and mechanism of interleukin-1 beta converting enzyme. *Nature* **370**, 270-275.

Zhang, R., Humphreys, I., Sahu, R. P., Shi, Y. and Srivastava, S. K. (2008) In vitro and in vivo induction of apoptosis by capsaicin in pancreatic cancer cells is mediated through ROS generation and mitochondrial death pathway. *Apoptosis* **12**, 1465-1478.